Volume 27
Number 31
21 August 2025
Pages 9283-9608

Green Chemistry

Cutting-edge research for a greener sustainable future

rsc.li/greenchem

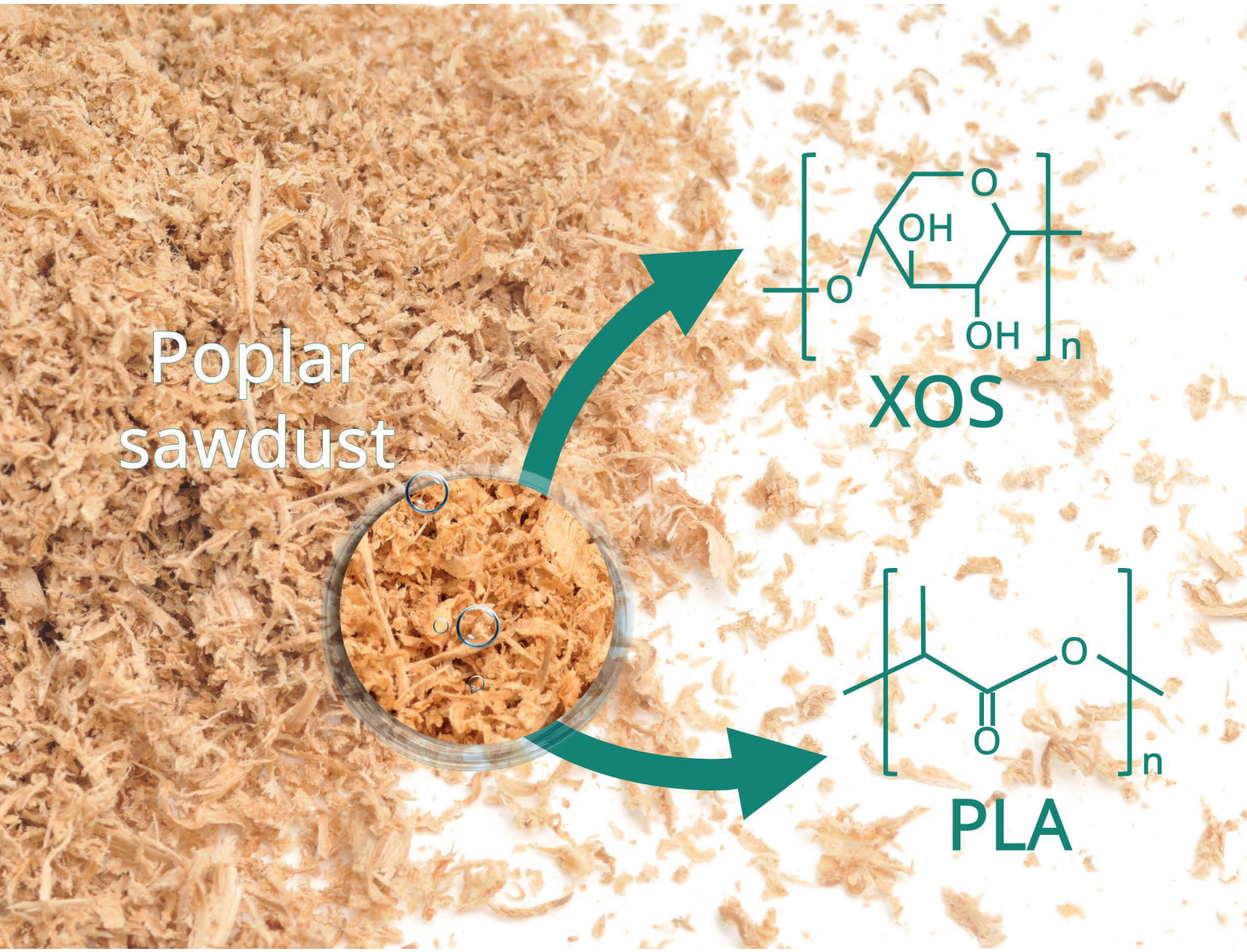

ISSN 1463-9262

ROYAL SOCIETY OF CHEMISTRY

PAPER

Caoxing Huang, Kai Lan *et al.*

Environmental feasibility of sustainable co-production of xylooligosaccharides and bioplastic from poplar sawdust

25 YEARS ANNIVERSARY

Green Chemistry

PAPER

View Article Online
View Journal | View Issue

Cite this: *Green Chem.*, 2025, **27**, 9480

Environmental feasibility of sustainable co-production of xylooligosaccharides and bioplastic from poplar sawdust†

Xiaoxue Zhao,[a] Ruolin Li,[a] Qiang Yong,[a] Caoxing Huang *[a] and Kai Lan *[b]

Received 28th March 2025,
Accepted 9th June 2025

DOI: 10.1039/d5gc01539a

rsc.li/greenchem

The upcycling of biomass waste into high-value bioproducts represents a significant shift away from low-value treatment methods, enhancing the circular bioeconomy. This study presents a cradle-to-gate life-cycle assessment (LCA) for the large-scale co-production of xylooligosaccharides (XOS) and polylactic acid (PLA) from poplar sawdust. The LCA was integrated with process models supported by experimental work. Various pretreatment conditions were investigated, including scenarios with different acetic acid concentrations (*i.e.*, 3%, 5%, and 7%) and a baseline without acetic acid. Our results show that the life-cycle global warming potential (GWP) of producing 1 dry kg of XOS is −3.3, 14.0, 19.9, and 49.9 $kgCO_2e$ for the cases without acetic acid, and with 3%, 5%, and 7% acetic acid, respectively. Using acetic acid in pretreatment results in higher GWP, predominantly due to the acetic acid and $CaCO_3$ in pretreatment, and the materials for purifying the XOS. The results of other environmental impact categories follow the results of GWP. On the basis of treating 1 dry ton of poplar sawdust, co-producing XOS and PLA achieves a lower GWP than conventional landfilling across scenarios. Only pretreatment without acetic acid can reach a lower GWP than landfilling with landfill gas recovery.

Green foundation

1. This work develops a life-cycle assessment for large-scale production of xylooligosaccharides and bioplastic from poplar sawdust under various pretreatment methods and conditions, supported by experimental work and green process design. This study advances green chemistry by integrally quantifying sustainability metrics of the various production pathways.
2. Although deploying acetic acid pretreatment leads to higher yields of xylooligosaccharides, we show that it largely increases the cradle-to-gate environmental impacts of xylooligosaccharides due to solvent recycling and product purification, compared to autohydrolysis. Higher acetic acid concentrations accentuate this trend.
3. The designed process described in this work can be utilized in future research to explore further the green processes for recovering solvent and prevent waste generation in systems based on green chemistry principles.

1. Introduction

In addressing the global energy crisis and escalating environmental pollution, the limitations and unsustainable nature of finite fossil fuel resources have become increasingly apparent.[1] Consequently, the transition to sustainable and renewable green energy and material resources has emerged as a critical strategy for global energy development. Lignocellulose, one of the most abundant renewable resources on Earth, offers multiple advantages, including widespread availability, renewability, and easy accessibility.[2,3] Its primary components, namely cellulose, hemicellulose, and lignin, can be converted into bioenergy products and biomaterials through biorefining, positioning it as a crucial pathway for advancing petroleum substitution strategies.[4,5] Thus, the efficient development and utilization of lignocellulosic biomass is pivotal to achieving long-term sustainable development goals.

Among various biomass feedstocks, forest resources are currently characterized by abundant plantation reserves but relatively low overall utilization efficiency, particularly for wood wastes.[6] The rational development and utilization of wood wastes for valuable bioproducts represent crucial research directions for future bioeconomy development. Among fast-growing hardwood species, poplar (*Populus trichocarpa*) stands out due to its rapid growth, strong adaptability, wide distri-

[a]*Co-Innovation Center of Efficient Processing and Utilization of Forest Resources, Nanjing Forestry University, Nanjing, 210037, China. E-mail: hcx@njfu.edu.cn*
[b]*Department of Forest Biomaterials, North Carolina State University, Raleigh, NC 27695, USA. E-mail: klan2@ncsu.edu*

† Electronic supplementary information (ESI) available. See DOI: https://doi.org/10.1039/d5gc01539a

bution, and high economic value. China possesses the largest area of poplar plantations in the world, with approximately 10 million hectares under cultivation and a total standing volume of 549 million m^3.[7,8] Currently, poplar is primarily used to produce plywood and flooring. The waste generated during poplar wood processing is often disposed of through landfill or burning, leading to underutilization of this waste, which also poses potential environmental concerns.[9] Poplar sawdust typically contains approximately 42%–49% cellulose, 20%–35% hemicellulose, and 20%–25% lignin.[8] From a biorefinery perspective, the high cellulose content in poplar can be converted into high-value biomaterials *via* pretreatment, enzymatic hydrolysis, and chemical or biochemical conversion processes.[10] However, challenges such as the feasibility of pretreatment technologies, high enzyme costs, and various inhibitory factors during enzymatic hydrolysis significantly hinder the viability of utilizing the poplar sawdust. To address these issues, graded conversion technologies for lignocellulosic components have gained significant attention. Hemicellulose, the second most abundant carbohydrate resource in nature, can be hydrolyzed into high-value sugar derivatives.[11] Among these, xylooligosaccharides (XOS) are important degradation products of hemicellulose. Due to their unique physicochemical properties and physiological functions, XOS is commonly used in probiotics, functional foods, and animal feed as alternatives to antibiotics, making them highly promising for commercial development.[12] Therefore, implementing a hemicellulose-first strategy, separating hemicellulose from poplar waste and converting it into XOS, could offset the costs of pretreatment and enzymatic hydrolysis in the biorefinery process. This approach presents an effective solution to enhance the economic viability of biorefining poplar sawdust.

XOSs, also known as xylooligomers, are functional oligosaccharides composed of typically 2 to 6 xylose units linked by β-1,4-glycosidic bonds. The primary bioactive components of XOS include xylobiose (X2), xylotriose (X3), xylotetraose (X4), xylopentaose (X5), and xylohexaose (X6).[13] XOS exhibits a variety of unique physiological functions, including selectively promoting the growth of gut probiotics, reducing cholesterol levels, exhibiting antioxidant properties, and enhancing immune system function.[14] These characteristics make XOS widely applicable in various sectors, including food, nutraceuticals, pharmaceuticals, and animal feed. In 2023, the global market sales of XOS reached USD 26.37 million, and are projected to grow to USD 32.26 million by 2030, reflecting a compound annual growth rate (CAGR) of 3.02%.[15] XOS products are primarily marketed in forms such as powder with purities of 95%, 70%, 35%, and 20%, as well as 70% syrup. Depending on purity, the market price of XOS prebiotics can range from USD 25 to 50 per kg.[16] By 2032, the global XOS market is expected to reach approximately USD 139 million, with North America and Europe being the primary markets. The CAGR during this period is estimated at 7%.[17,18] The United States currently leads global XOS consumption, followed by Germany and Japan, with market shares of 34%, 13%, and 1.5%, respectively.[14] As consumer awareness of health increases and the application areas of XOS expand, sustained market growth is anticipated in the coming years.

To meet growing market demand, effective methods for the industrial-scale production of XOS with high yields are emerging.[19] Various techniques, including physical, chemical, physicochemical, and biological pretreatments, can be employed for XOS preparation.[20] Among these, hydrothermal pretreatment (also known as autohydrolysis)[16] is one of the most commonly used methods for preparing XOS. Currently, hydrothermal pretreatment is widely applied to both herbaceous and woody biomass for XOS production. For example, Fang *et al.*[21] used birch wood as a feedstock and performed hydrothermal pretreatment at 170 °C for 70 minutes, achieving an XOS yield of 51.4% relative to the original xylan content. Zhang *et al.*[22] conducted hydrothermal pretreatment of sugarcane bagasse at 200 °C for 10 minutes, achieving an XOS yield of 50.35%. Neto *et al.*[23] applied hydrothermal pretreatment to eucalyptus at 160 °C for 65 minutes, with an XOS yield of 42.6%. Due to its advantages, such as not requiring chemical reagents other than water and demonstrating low corrosiveness towards equipment, hydrothermal pretreatment is potentially considered an environmentally friendly method.

In addition to hydrothermal methods, acetic acid pretreatment is another commonly used method for preparing XOS.[24] During acetic acid pretreatment, the degradation of hemicellulose is primarily achieved through an acid-catalyzed hydrolysis mechanism. The acetic acid added to the pretreatment system directly creates an acidic environment.[25] In addition, the acetyl group of hemicellulose is hydrolyzed at high temperature, releasing free acetic acid and forming an autocatalytic effect, which facilitates selective degradation of hemicellulose into soluble oligosaccharides and monosaccharides.[25] Zhang *et al.* pretreated corncob with acetic acid at pH 2.7 and 150 °C for 30 min, which resulted in an XOS yield of 45.9%.[26] Wen *et al.* treated poplar with 5% acetic acid at 170 °C for 30 min, achieving a higher XOS yield of 55.8%.[24] Meanwhile, Zhou *et al.* used 10% acetic acid to treat sugarcane bagasse at 150 °C for 45 min, achieving an XOS yield of 39.1%.[27] XOS produced by acetic acid pretreatment typically contains a significant proportion of compounds with a higher degree of polymerization (DP > 6), which often requires further enzymatic hydrolysis to release more low-DP XOS with improved prebiotic functionality and bioavailability. Overall, acetic acid pretreatment has demonstrated notable effectiveness in XOS production, and ongoing research is being focused on optimizing both the pretreatment conditions and subsequent enzymatic steps to enhance XOS yield and application potential.

After pretreatment, further hydrolysis of xylan using xylanase enables the low-cost and highly efficient production of XOS.[27] Due to differences in lignocellulosic sources and the physicochemical properties of hemicellulose, the synergistic action of xylanase and other enzymes is often required.[28] Successful enzymatic production of XOS depends on several critical factors, including the type and structural complexity of hemicellulose in the raw material, the specific enzymes

employed, and the enzyme composition ratio. These parameters must be carefully optimized to maximize XOS yield and efficiency. In summary, employing appropriate methods to break the dense structure of poplar is crucial for achieving higher XOS extraction yields and enabling sustainable production. Different preparation pathways and methods will directly influence the final XOS yield, energy demand, and material consumption, and further impact the environmental performance of XOS.

Life-cycle assessment (LCA) is a standardized tool to evaluate the environmental performance of a product or process throughout its life cycle.[29–31] LCA has been widely applied for emerging bioproducts to evaluate their environmental feasibility and inform green process design.[32–34] Previous studies that have employed the LCA for XOS production from various feedstocks are limited.[35–37] Van Heerden *et al.* developed the LCA and economic analysis for the biorefinery producing 1,3-propanediol and XOS from sugarcane.[35] The reported life-cycle greenhouse gas (GHG) emission values were 9.21–11.4 $kgCO_2e$ per kg XOS produced.[35] González-García *et al.* conducted the LCA for a biorefinery generating ethanol and XOS from brewery waste and reported the life-cycle GWP to be 4.21 $kgCO_2e$ per kg XOS produced.[36] Lopes *et al.* adopted the LCA to evaluate the life-cycle environmental impacts of small-scale biorefineries in varied locations that produced isobutene (as the major product) and XOS from agricultural residues.[37] The authors reported that the biorefinery in Chile achieved lower environmental impacts.[37] However, few previous LCA studies have investigated the life-cycle environmental implications of XOS production from woody biomass. At the same time, since previous studies have extensively studied how acetic acid pretreatment could enhance XOS production, it is important to know how these various pretreatment methods and conditions can impact environmental performance. This critical aspect has not been fully explored, either. Moreover, the key drivers for the life-cycle environmental impacts of the XOS production system have not been fully identified. Additionally, the key processes of previous studies were not integrally coupled with experimental work and results.

To address the knowledge gaps, this study develops a cradle-to-gate LCA for large-scale XOS production from poplar sawdust under various pretreatment methods and conditions to attain animal feed-grade quality. This LCA is integrated with experimental work and rigorous process models that provide detailed mass and energy balance data. The byproduct converted from separated cellulose is selected as polylactic acid (PLA). PLA is chosen as a promising bioplastic with an increasingly promising future to displace traditional fossil-based plastics.[38–40] This study designs an integrated biorefinery system that can pretreat biomass, produce XOS, purify XOS, and co-produce PLA. Four scenarios are developed to explore the impacts of pretreatment methods and pretreatment conditions on the life-cycle environmental impacts. A sensitivity analysis is conducted to present the key drivers of the life-cycle environmental results. This research reports the detailed experimental results obtained under various pretreatment conditions, and the designed biorefinery processes that are technically feasible and environmentally friendly to produce and purify XOS and PLA at a large scale with mature technologies and equipment. This biorefinery design is further simulated and validated in a rigorous process model to provide detailed mass and energy balance data. It is our hope that this LCA study clarifies whether acetic acid pretreatment for XOS production is green or not at the current stages of technology, along with identifying key contributors and trade-offs in the system. These contributors can be the main direction for future research to investigate greener processes of this system, with trade-offs better informing the industry of process design and control. This study shows how LCA can be integrated with green process design to inform and improve the technical selections of pretreatment methods and conditions.

2. Materials and methods

Fig. 1 displays the research approach of this study. The detailed biorefinery diagram and LCA system boundary are exhibited in Fig. 2. The experimental data of key reactions (*e.g.*, pretreatment, enzymatic hydrolysis for XOS and glucose) were based on the experimental results.[41–44] Along with the processes for the PLA production from glucose based on the data from published literature,[45] a rigorous process simulation model was constructed using Aspen Plus software. This process simulation model generated the mass and energy balances needed by the LCA model as life-cycle inventory (LCI) data. The LCA model was constructed by following ISO 14040 and 14044 standards (see section 2.3).[31,46] Scenario analysis explored the impacts of pretreatment conditions and key parameters. Sensitivity analysis identified the key drivers of the results (see section 2.4). The sections below describe detailed methods.

2.1. Feedstock characterization

Poplar (*Populus trichocarpa*) sawdust was adopted as the feedstock in this study. The chemical composition was determined by following the methods proposed by the U.S. National Renewable Energy Laboratory (US NREL).[45] The feedstock composition contains 44.7% glucan, 17.1% xylan, 25.7% lignin, 1.8% extractives, 0.6% ash, and 10.1% other impurities. The moisture content (w.b.) of poplar sawdust after drying was 10.9%.

2.2. Biorefinery processes

Fig. 2 depicts the system diagram of the biorefinery and the system boundary of the LCA. The biorefinery was designed at the capacity of 100 dry t per day. The biorefinery consists of five areas, including A100 feedstock handling, A200 pretreatment, A300 XOS production, A400 polylactic acid production, and A500 CHP plant. The PLA production area followed the design of the Greenhouse Gases, Regulated Emissions, and Energy use in Technologies Model (GREET) produced by the

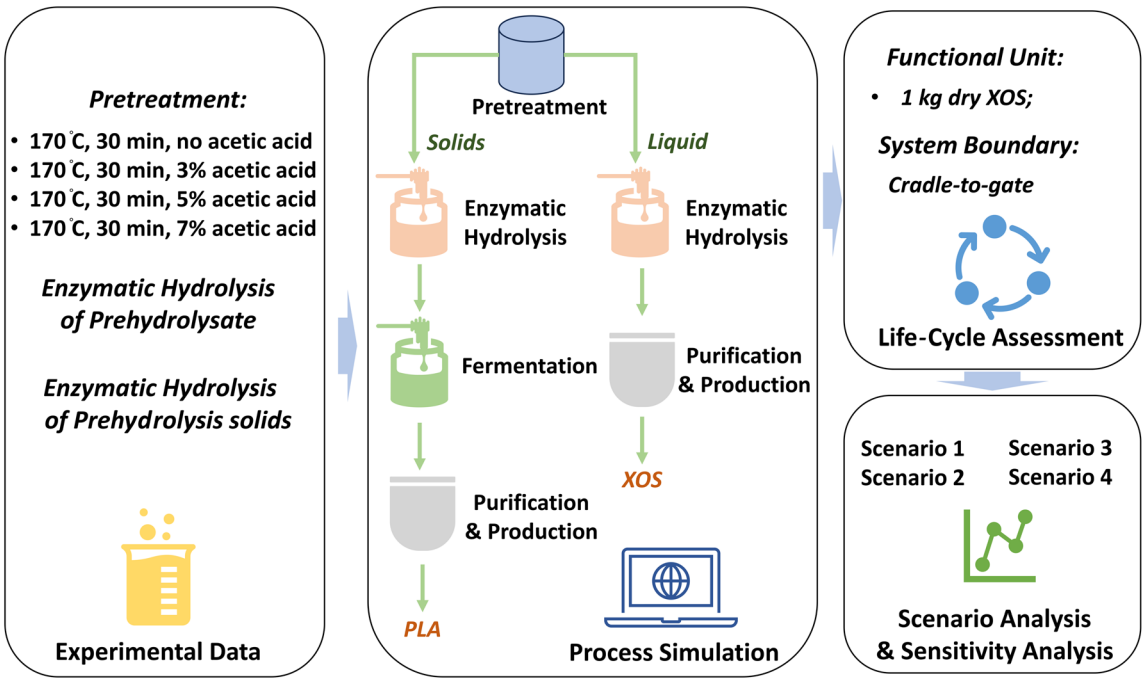

Fig. 1 The summarized research approach and biorefinery scheme.

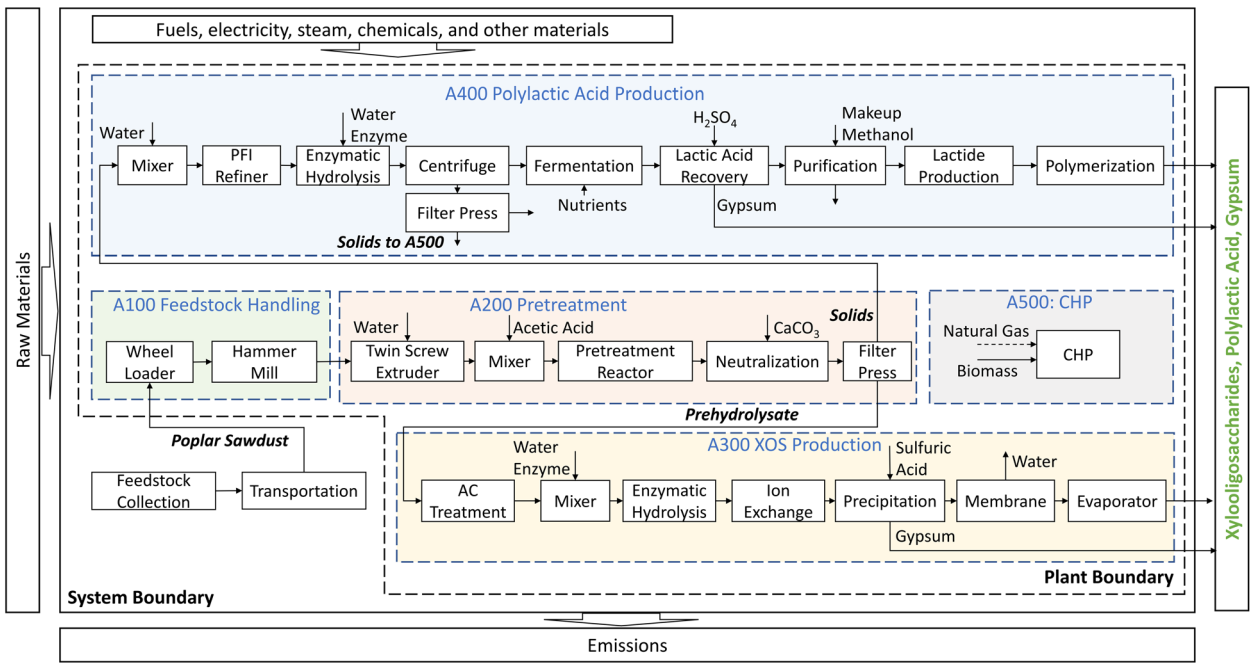

Fig. 2 The system boundary of life-cycle assessment and the flow diagram of the biorefinery.

U.S. Argonne National Laboratory.[47] Set out below are the details of each area.

2.2.1. Feedstock handling. The poplar sawdust was stored indoors. Poplar sawdust was first air dried, and then milled to a particle size between 20 and 80 mesh (0.18 mm–0.85 mm).[41]

2.2.2. Pretreatment. The milled poplar sawdust was conveyed to pretreatment. A twin-screw extruder was deployed to perform the extrusion process because of its cost efficiency and the improvement of sugar recovery.[48] In the extrusion process, while the twin-screw extruder was operated, acetic acid solution was added to achieve a solid-to-liquid ratio of

1 : 10. The solids loading was selected based on prior experimental optimization and literature precedents, primarily to facilitate effective heat and mass transfer, minimize viscosity-related mixing issues, reduce the accumulation of inhibitors, and control xylan degradation to xylose.[41,49] Hydrolysis pretreatment with acetic acid has been widely used in XOS production as a low-cost unit process.[41,42] This pretreatment can degrade xylan into soluble oligomers under a controlled operational temperature (typically 140–200 °C).[50] In this study, to explore the impact on the final results of pretreatment with acetic acid of different concentrations, several scenarios were analyzed, including (1) 170 °C, 30 min without acetic acid (autohydrolysis); (2) 170 °C, 30 min, and 3% acetic acid concentration; (3) 170 °C, 30 min, and 5% acetic acid concentration; and (4) 170 °C, 30 min, and 7% acetic acid concentration. These scenarios were selected based on previous experimental data and studies.[41,42] The detailed reactions and corresponding conversion rates were generated based on each experiment and the results are recorded in Table 1. After the pretreatment, $CaCO_3$ was added to neutralize the solution. The required amount of $CaCO_3$ varied depending on the acidity in the different pretreatment solutions. The filter press was then used to separate the liquids and solids. The liquid phase was transferred to the XOS production area. The filter cake (solids) containing glucan, lignin, and other insoluble solids was sent to the PLA production area.

2.2.3. XOS production. Although the solution was neutralized with $CaCO_3$, residual furfural and hydroxymethylfurfural (HMF) were still present. To further reduce their concentrations and minimize potential inhibitory effects on subsequent processing, the liquid phase of the pre-hydrolysate was treated using activated carbon to remove phenolics, mainly furfural and HMF.[16] During treatment with activated carbon, a sugar loss of 20% is assumed in this study.[51] Enzymatic hydrolysis was then deployed to convert high-DP XOS and low-DP xylan into xylobiose and xylotriose, which intestinal bifidobacteria preferentially utilize over high-DP XOS.[52] The *endo*-xylanase enzymatic hydrolysis is conducted at 50 °C for 48 hours with acetate buffer at pH 4.8.[52] The enzymatic hydrolysis adopted the *endo*-xylanase at a load of 17 mg g^{-1} XOS solution.[52,53] The detailed reactions and conversion rates were determined *via* experiment and are shown in Table 2. Ion exchange was then deployed to purify the stream using ion exchange resin washed with NaOH. After the ion exchange, the stream was mixed with sulfuric acid to precipitate gypsum. Separation using the ultrafiltration membrane concentrated the stream to 20% solids.[54] Finally, a spray dryer was deployed to produce XOS powder.[55] The final XOS content of the product, including X2–X6 and soluble low-DP xylan, for the purpose of generating animal feed, is above 32%.

2.2.4. Polylactic acid production. The filter cake was mixed with water to a consistency of 10% and subjected to the Papir Forsknings Institutet (PFI) milling. After grinding, enzymatic hydrolysis was conducted to convert the glucan into fermentable sugars for PLA production. Enzymatic hydrolysis was conducted at 50 °C for 72 h with cellulase (Cellic® CTec2 from Novozymes, USA) loaded at 8 mg g^{-1} glucan.[41] The solid loading was 5% (w/v) for enzymatic hydrolysis in sodium citrate buffer (pH 4.8, 0.05 M).[41,42] The solid loading value was selected based on previous experimental work for the enzymatic hydrolysis of acetic acid-pretreated poplar sawdust, where superior hydrolysis performance was demonstrated with 5% solid loading.[41,42] The detailed reactions and conversion rates were derived from the experiment and are shown in Table 3.[41]

After the enzymatic hydrolysis, centrifugation was employed to eliminate the residual dense components, including lignin, glucan, xylan, and other substantial oligomers.[56] The solids were then filtered and combusted in the CHP plant for power and heat supply for the biorefinery. The extracted sugars were fermented into L-lactic acid using the bacterium *Bacillus coagulans*.[47] Detailed methodologies for lactic acid fermentation were designed in accordance with the GREET model.[47] The nutrient stream required for seed fermentation was sterilized at 135 °C for a duration of 2 min, followed by cooling to 42 °C.[47] Next, the inoculum was introduced at a volume percentage of 10% of the sugar solution. The combination of sugar and nutrient solutions was sterilized at 135 °C for 2 min

Table 1 Pretreatment reactions and yield

		% final yield			
Reaction	Reactant	Scenario 1	Scenario 2	Scenario 3	Scenario 4
$(Xylan)_n + n/2\ H_2O \rightarrow n/2\ C_{10}H_{18}O_9$ (X2)	Xylan	1.08%	7.70%	10.03%	7.41%
$(Xylan)_n + n/3\ H_2O \rightarrow n/3\ C_{15}H_{26}O_{13}$ (X3)	Xylan	0.97%	5.94%	8.35%	5.82%
$(Xylan)_n + n/4\ H_2O \rightarrow n/4\ C_{20}H_{34}O_{17}$ (X4)	Xylan	2.23%	7.20%	9.31%	5.32%
$(Xylan)_n + n/5\ H_2O \rightarrow n/5\ C_{25}H_{42}O_{21}$ (X5)	Xylan	0.96%	3.05%	4.72%	1.46%
$(Xylan)_n + n/6\ H_2O \rightarrow n/6\ C_{30}H_{50}O_{25}$ (X6)	Xylan	1.38%	3.22%	3.75%	1.35%
$(Xylan)_n \rightarrow$ low DP xylan[a]	Xylan	31.72%	12.37%	17.20%	10.22%
$(Xylan)_n + n\ H_2O \rightarrow n$ xylose	Xylan	4.30%	5.38%	15.06%	25.81%
$(Glucan)_n + n\ H_2O \rightarrow n$ glucose	Glucan	1.71%	3.76%	4.30%	5.91%
$(Xylan)_n \rightarrow n$ furfural $+ 2n\ H_2O$	Xylan	N.D.	0.26%	0.42%	0.54%
$(Lignin)_n \rightarrow n$ soluble lignin	Lignin	1.71%	2.92%	4.40%	5.07%

[a] Low-DP xylan: soluble xylan with a low degree of polymerization (DP > 6) in pre-hydrolysate.

Table 2 Enzymatic hydrolysis reactions and yield for the prehydrolysate[41,43]

Reaction	Reactant	% final yield			
		Scenario 1	Scenario 2	Scenario 3	Scenario 4
$(Xylan)_n + n/2\ H_2O \rightarrow n/2\ C_{10}H_{18}O_9$ (X2)	Low-DP xylan	14.52%	15.06%	18.60%	16.02%
$(Xylan)_n + n/3\ H_2O \rightarrow n/3\ C_{15}H_{26}O_{13}$ (X3)	Low-DP xylan	9.14%	12.66%	10.91%	7.86%
$(Xylan)_n + n/4\ H_2O \rightarrow n/4\ C_{20}H_{34}O_{17}$ (X4)	Low-DP xylan	2.69%	3.41%	7.31%	5.66%
$(Xylan)_n + n/5\ H_2O \rightarrow n/5\ C_{25}H_{42}O_{21}$ (X5)	Low-DP xylan	N.D.	0.20%	0.55%	N.D.
$(Xylan)_n + n/6\ H_2O \rightarrow n/6\ C_{30}H_{50}O_{25}$ (X6)	Low-DP xylan	N.D.	N.D.	1.65%	N.D.
$(Xylan)_n \rightarrow n$ xylose $+ n\ H_2O$	Low-DP xylan	6.99%	9.14%	17.74%	27.96%

Table 3 Enzymatic hydrolysis reaction and yield for the pretreatment solids

Reaction	Reactant	% converted to product			
		Scenario 1	Scenario 2	Scenario 3	Scenario 4
$(Glucan)_n + n\ H_2O \rightarrow n$ glucose	Glucan	47.71%	56.83%	60.14%	72.52%

prior to fermentation. The fermentation was conducted at 42 °C over a period of 72 h. $CaCO_3$ was incorporated to maintain a pH level of 6.5. The final solution contained approximately 8% calcium lactate and was sent for purification. The fermentation was performed in batch mode.[47] The detailed reactions associated with lactic acid production are documented in Table 4 based on previous patents and validated studies.[47,57,58] In this study, the solids are filtered after enzymatic hydrolysis in order to be sent to the CHP plant. This is due principally to three motivations. First, the current focus of the major commercial producers and research in the literature is mainly on sugar fermentation.[47,59] It is still unknown how the solids will influence the lactic acid yield. Second, it is easier to yield pure gypsum (see below) after sulfuric acid is added to recover lactic acid. Third, with the stream mass and volume reduced, the energy demand of handling the stream in fermentation will be less. Future research can investigate further lactic acid fermentation with solids under various pretreatment conditions.

Lactic acid was recovered by adding sulfuric acid to form calcium sulfate and dilute the lactic acid solution. The filter press separated the gypsum formed from the liquid phase that mainly contained dilute lactic acid, nutrients, and the remaining sugars. To produce PLA from dilute lactic acid, the indirect route *via* ring-opening polymerization was deployed because the major producers of PLA have adopted this route.[59–64] The detailed design of the purification process followed that of Bapat *et al.*[65] and Dunn *et al.*[47] There are three major steps in the purification process that are followed in the continuous mode. First, the falling-film evaporator evaporates the lactic acid solution to approximately 50 wt%. Second, the solution is esterified with methanol to produce methyl lactate and water.[47,65] The reaction is conducted on a reactive distillation column. The methyl lactate solution is passed through the distillation columns to reach approximately 90–95 wt%.[65] Residual methanol is recovered using a distillation column. Third, the highly concentrated methyl lactate solution is hydrolyzed to release lactic acid and methanol. This solution is then distilled to recover the lactic acid (99 wt%).[66] The overhead is then recycled back into the methanol recovery column. From polymer-grade lactic acid to PLA, the ring-opening polymerization route has been adopted in this study as it is the most widely used method.[59,63,67] Lactide is formed from polymer-grade lactic acid and is then distilled into pure lactide and polymerized into PLA.[38,63]

Table 4 Lactic acid yield

Reaction	Reactant	% final yield
Glucose → 2 lactic acid	Glucose	98.0%
3 xylose → 5 lactic acid	Xylose	95.0%

2.2.5. Combined heat and power plant. The CHP plant design follows the U.S. NREL report.[68] The separated filter cake is combusted. The boiler generates superheated steam at 60 atm and 454 °C with 80% efficiency.[68] The superheated steam then passes through multistage turbines for power generation. In this study, low-pressure steam at 13 atm and 268 °C is used to provide heat for unit operations. Electricity is generated by the turbines in a CHP plant and supplies power to the entire plant. Excess electricity is sold to the grid. If the heat supply from biomass alone is insufficient, natural gas is combusted as a supplemental source.

2.3. Life-cycle assessment model

This study adopted a cradle-to-gate LCA to quantify the life-cycle environmental impacts of the XOS produced from poplar sawdust, following the ISO standard 14040 series.[31,46] The system boundary is displayed in Fig. 2, including feedstock collection, transportation, and production. The upstream burdens of producing chemicals, materials, fuels, and electricity have been included. Since poplar sawdust was regarded as

waste, the upstream burdens of generating poplar sawdust were assumed to be zero. The functional unit was selected as 1 dry kg XOS produced for animal feed. At the same time, this study normalized the results to the basis unit of 1 dry t poplar sawdust to compare it with current waste treatment methods. The mass and energy balance data for LCI analysis were generated from the process models as described above. Other LCI data for the background processes were derived from the literature, the ecoinvent 3.10 cut-off database, and the GREET model created by the U.S. Argonne National Laboratory.[69,70] As the system can contain more than one product (*i.e.*, XOS, PLA, gypsum), it is necessary to identify the share of the environmental burden attributed to XOS. Following the allocation procedure required by ISO standards 14040 and 14044,[31,46] allocation should be avoided by dividing the unit process, if possible, or system expansion as the first step. Since it is very hard to justify and split every unit process in the biorefinery to allocate the burden among the three products, system expansion was employed based on these ISO guidelines.[31,46] To test the sensitivity of the results with respect to the allocation method, this study also extensively used economic allocation to generate the results as the third step of the allocation procedure according to the ISO guidelines.[31,46] The mass allocation, as the second step of the allocation procedure in the ISO guidelines, is not suitable for the system in this study, based on two reasons. One is that the gypsum byproduct yield is much higher than that of XOS and PLA in some scenarios (see section 3.1) and leads to the environmental burden of XOS being too low; the second reason is the economic value of XOS ($6850 per t at feed grade)[14,71–73] is much higher than PLA ($2800 per t)[74] and gypsum ($72.4 per t),[75] where using mass allocation is not able to reflect the major purpose of the biorefinery.

To better provide the comparative implications of conventional waste treatment methods, the GWP of disposing poplar sawdust through landfill (mainly CH_4 and CO_2) was modeled following the Intergovernmental Panel on Climate Change (IPCC) First Order Decay (FOD) method for the 100-year decay process (see ESI Table S1† for details and parameter values).[76] Landfill gas (LFG) recovery is becoming increasingly attractive,[77] since landfill gas has energy value with a high climate change contribution due to CH_4.[77,78] In this study, we also include two counterfactual scenarios: landfill with and without LFG recovery to compare with our XOS production pathways.

In the life-cycle impact assessment (LCIA), TRACI 2.1 from the US Environmental Protection Agency was selected to assess the life-cycle environmental impacts with the GWP-100 factors from the IPCC AR6 report.[79,80] The LCIA impact categories included GWP, acidification, human health – carcinogenics, human health – non-carcinogenics, eutrophication, fossil fuel depletion, ozone depletion, smog formation, ecotoxicity, and respiratory effects.[79,80] In this study, the biogenic carbon of the XOS product was assumed to be finally oxidized into CO_2. Hence, this study assumed that the biogenic carbon was neutral on the product-level.

2.4. Scenario analysis

To explore the impacts of different pretreatment conditions on the environmental impacts of the XOS products, we established four scenarios, as mentioned above. Scenario 1 utilized water without acetic acid (autohydrolysis) to pretreat the feedstock. Scenarios 2, 3, and 4 deployed 3%, 5%, and 7% acetic acid solution, respectively, for pretreatment.

3. Results and discussion

3.1. Technical performance of the biorefinery

To further evaluate the effect of acetic acid concentration during the pretreatment stage on the conversion of poplar hemicellulose into XOS, the technical performance of the biorefinery producing XOS or PLA from poplar sawdust was evaluated under four different scenarios, as summarized in Table 5. All values presented in Table 5 are based on a daily processing capacity of 100 dry t of feedstock.

For the product yield, scenario 3 with acetic acid pretreatment demonstrates significantly higher productivity of total XOS compared to scenarios 1, 2, and 4. For example, the total XOS yield in scenario 1 is 4.6 t per day. As the acetic acid concentration increases to 3%, 5%, and 7%, the total XOS content in the hydrolysate rises to 5.0 t, 6.6 t, and 3.8 t per day, respectively. This trend may be attributed to the enhanced degradation of poplar hemicellulose into oligosaccharides with increasing acetic acid concentration. However, when the concentration of acetic acid exceeds 5% at a fixed solid–liquid ratio of 1 : 10, xylan in the raw materials is more readily degraded to xylose or even to furfural and other degradation products, which inhibits further hemicellulose degradation.[81] This is consistent with the xylose yield shown in Table 5, where scenario 4 has a higher xylose content in the hydrolysis products compared to that in scenarios 1, 2, and 3. Compared with conventional XOS production from agricultural residues such as corncob, which typically yields 5.8–14.0 t per 100 dry t feedstock depending on process conditions, the XOS yield from poplar sawdust in this study (up to 6.6 t) is competitive.[26,82] Given that woody biomass like poplar sawdust contains lower hemicellulose content and presents greater recalcitrance, the result highlights its potential as a supplementary feedstock for sustainable XOS production. Typically, XOS of low-degree of polymerization (X2–X6) exhibits higher biological activity and economic value compared to XOS of high-degree of polymerization.[83] As indicated in Table 5, scenario 3 demonstrates much higher productivity of X2–X6 than scenarios 1, 2, and 4. Specifically, the X2–X6 yield in scenarios 1, 2, and 4 is 2.0, 4.1, and 3.3 t per day, respectively, while scenario 3 yields 5.7 t per day. Furthermore, the ratio of X2 to X3 is an important indicator for evaluating the XOS activity, and this ratio is influenced by acetic acid concentration. As shown in Table 5, the proportion of X2–X3 in scenario 3 is higher than that in scenarios 1, 2, and 4, that is, the X2–X3 yield in scenarios 1, 2, and 4 is 1.3, 2.3, and 2.1 t per day, respectively, compared to 3.2 t per day in scenario 3. This

Table 5 Mass and energy balances of the biorefinery

	Scenario 1	Scenario 2	Scenario 3	Scenario 4
Pretreatment condition	No acetic acid	3% acetic acid	5% acetic acid	7% acetic acid
Material input (t per day)				
Dry feedstock	100.0	100.0	100.0	100.0
Water	2540.2	2610.1	2582.4	2671.5
Acetic acid	0.0	30.8	52.5	75.1
$CaCO_3$	12.5	40.3	59.2	80.9
Ion exchange resin	0.7	4.1	6.9	9.3
Activated carbon	0.0	0.1	0.2	0.3
H_2SO_4	12.3	37.2	54.5	74.4
NaOH	12.3	33.0	47.2	64.0
Methanol	6.6	7.8	8.3	10.0
Glucose	0.3	0.4	0.4	0.5
Nitrogen gas	3.5	4.1	4.3	5.1
Sodium acetate	0.6	0.7	0.8	0.9
Sodium chloride	6.6	7.7	8.2	9.7
Yeast extract	11.5	13.4	14.2	16.9
Energy input				
Electricity (MWh per day)	4.6	6.8	8.9	9.5
Output (t per day)				
XOS product				
X2	0.8	1.3	1.8	1.2
X3	0.5	1.0	1.4	0.9
X4	0.4	1.0	1.4	0.8
X5	0.1	0.4	0.6	0.2
X6	0.2	0.4	0.5	0.2
Low DP xylan	2.6	0.9	1.0	0.6
Xylose	0.9	0.9	2.6	4.1
Glucose	0.6	1.4	1.6	2.2
Other	0.3	0.9	1.5	1.9
Total XOS	4.6	5.0	6.6	3.8
PLA	11.5	13.6	14.4	17.3
Gypsum	17.0	51.7	75.6	103.2
Wastewater	2510.2	2610.7	2607.9	2712.4

can be attributed to the increased pretreatment intensity, where the removal of acetyl groups from cellulose forms more acetic acid, leading to a decrease in the system's pH.[84] This accelerates the degradation of XOS components with a degree of polymerization greater than three, thus increasing the content of X2 and X3. In Table 5, the product of high-degree polymerization XOS (low-DP xylan) for scenarios 1, 2, 3, and 4 are 2.6, 0.9, 1.0, 0.6 t per day, respectively. These results suggest that scenario 3 not only achieved the highest yield of low-DP XOS but also benefited from the addition of xylanase, which enhanced the hydrolysis of longer-chain oligosaccharides, further increasing the production of X2 and X3.[41]

It was further observed that the yield of polylactic acid (PLA) increased with rising acetic acid concentrations during pretreatment. As shown in Table 5, the daily PLA yields for scenarios 1, 2, 3, and 4 were 11.5, 13.6, 14.4, and 17.3 t, respectively, indicating a positive correlation between acetic acid concentration and PLA production. This trend contrasts with that of the XOS yield. Overall, energy consumption in all four scenarios increases with the concentration of acetic acid from Table 5. However, it should be noted that XOS is temperature-sensitive and prone to degradation, and distillation is not suitable for XOS purification, as it may affect the quality of the final product. Nevertheless, the results of this study still demonstrate the efficacy of acetic acid pretreatment as a pivotal process for the valorization of poplar sawdust into high-value-added bioproducts. In conclusion, the combined approach of acetic acid pretreatment and xylanase hydrolysis is efficient for the objective of the degradation of hemicellulose into XOS from poplar sawdust.

3.2. Life-cycle GWP of 1 kg XOS

The cradle-to-gate GWP of 1 kg XOS produced by the biorefinery is depicted in Fig. 3 by using the system expansion method. All the life-cycle stages are displayed together with detailed contributors to the results. All GWP values are presented on the basis of $kgCO_2e$ per kg XOS, in accordance with the current literature.[35–37] In Fig. 3, positive values indicate the GWP caused by GHG emissions, while the negative values represent potential GWP credits gained when byproducts replace market products. The total GWP of each scenario is marked as diamonds by summing all the GWP contributors.

Across the four scenarios, the total GWP per kg XOS value is lowest in scenario 1 at −3.3 $kgCO_2e$, with 14.0 $kgCO_2e$ in scenario 2, 19.9 $kgCO_2e$ in scenario 3, and 49.9 $kgCO_2e$ in scenario 4. These counterintuitive results reveal that deploying acetic acid pretreatment will increase the life-cycle GWP with increasing acetic acid concentration, in comparison with scenario 1 where autohydrolysis is deployed. Hence, the trade-off is identified here between GWP and XOS yield. Leveraging acetic

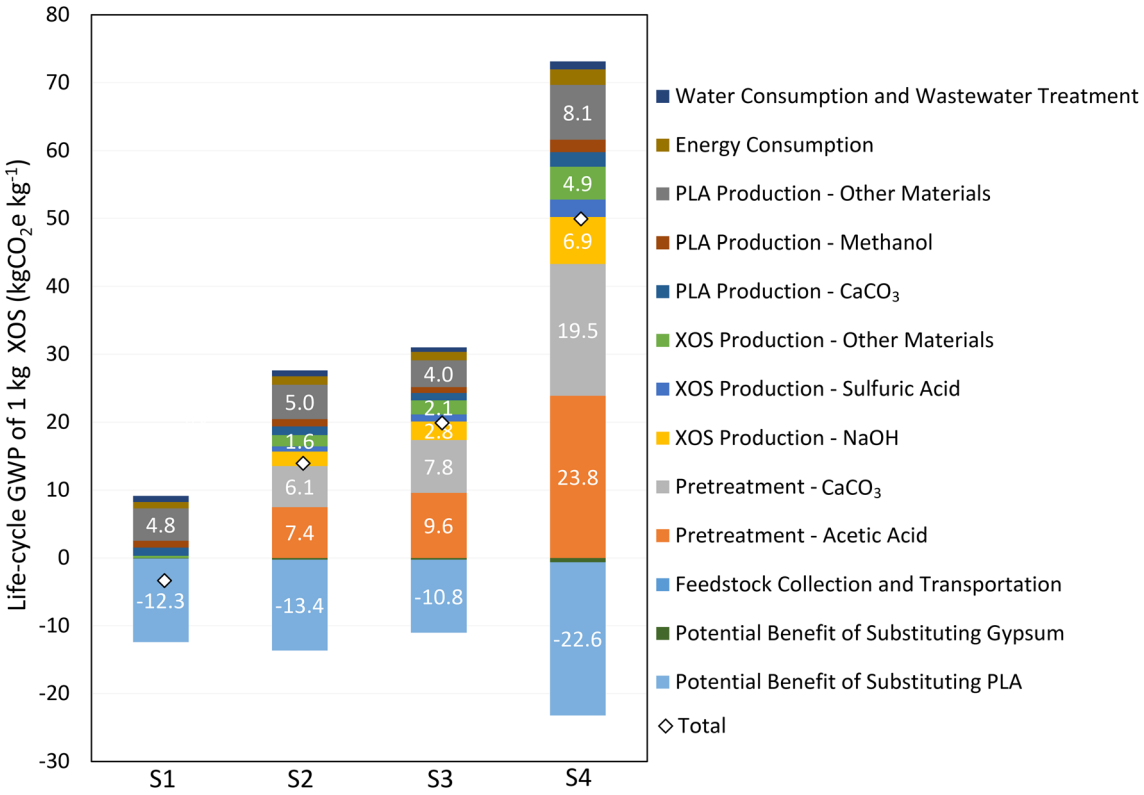

Fig. 3 The life-cycle GWP of 1 kg XOS in four scenarios.

acid pretreatment in scenarios 2 and 3 indeed increases the total XOS yield compared to scenario 1 (see Table 1) but harms the carbon aspects of the XOS produced. Current LCA literature on XOS reported 4.2–11.4 $kgCO_2e$ per kg XOS produced in various locations with various feedstocks and co-products.[35–37] This range is comparable to the GWP results of scenarios 1 and 2. However, the GWP results of XOS still rely highly on the detailed biomass feedstock, co-products, and production pathways.[35–37]

The highest value contributions to the GWP across scenarios 2–4 are derived from the acetic acid in pretreatment (orange bars in Fig. 3) and $CaCO_3$ in pretreatment (gray bars in Fig. 3). The GWP from acetic acid in pretreatment shows 7.4–23.8 $kgCO_2e$ with increasing acetic acid concentration in scenarios 2–4. Note that in scenario 4, the total XOS yield is lower than that in scenarios 2 and 3 and leads to the GWP per kg XOS basis being much higher than that in scenarios 2 and 3. At the same time, in order to neutralize the acetic acid, a large amount of $CaCO_3$ is used, resulting in 6.1–19.5 $kgCO_2e$ in scenarios 2–4 (including the CO_2 emission during neutralization). This result highlights the research needed to explore more efficient methods of recycling the acetic acid towards greener production. Currently, there are research efforts exploring the various advanced methods for recycling and purifying acetic acid from liquid following green chemistry principles, *e.g.*, solvent extraction *via* deep eutectic liquids or ionic liquids,[85] mechanical vapor recompression,[86] membrane separation,[87] and other technologies. If the acetic acid can be potentially recycled, then the neutralization process can be eliminated at the same time. However, these potential methods need to consider the fact that XOS is easy to degrade and sensitive to temperature, and consider the practical process design for sequential XOS purification.

Besides the major contributions from acetic acid and $CaCO_3$, other materials in PLA production (including sulfuric acid, nutrients, NaOH, and enzymes) follow the same trends as the main sources of GHG emissions (dark gray bars in Fig. 3), revealing a range of 4.8–8.1 $kgCO_2e$ across the four scenarios, increasing with higher acetic acid concentrations. $CaCO_3$ and methanol in PLA production account for 1.0–2.2 $kgCO_2e$ and 0.9–1.8 $kgCO_2e$, respectively. However, the GWP from PLA production is compensated for by the potential GWP benefits of substituting current market PLA production, shown as negative values in Fig. 3. Across the scenarios, the potential benefit of substituting market PLA production is −22.6 to −10.8 $kgCO_2e$. In scenario 1, this benefit is 12.3 $kgCO_2e$, which is higher than the GWP figures of all the GHG emission types, leading to the final −3.3 $kgCO_2e$ life-cycle GWP value. This result emphasizes the importance of upcycling biomass waste into high-value and carbon-intensive products. In this study, the life-cycle GWP of scenario 1 is negative (−3.3 $kgCO_2e$ per kg XOS). This is largely caused by

the potential benefits of substituting PLA, as the system expansion method is used. This result is sensitive to the carbon intensity of the current PLA and how much PLA is produced (see Fig. 6). If this potential benefit of substituting PLA (12.3 $kgCO_2e$ per kg XOS) decreases by 50%, the life-cycle GWP of XOS in scenario 1 will increase to 2.9 $kgCO_2e$ per kg XOS.

In the production of XOS, NaOH, sulfuric acid, and other materials contribute 0–6.9 $kgCO_2e$, 0–2.6 $kgCO_2e$, and 0.3–4.9 $kgCO_2e$, respectively. It is noticeable that, in scenario 1, since no acetic acid and calcium carbonate is used, NaOH for ion exchange and sulfuric acid for precipitation in XOS production will be zero. Compared to acetic acid pretreatment, the GWP of XOS and PLA production is still relatively small. Hence, the life-cycle GWP results demonstrate that coupling LCA with process design is critical to explore and improve the sustainability of the product.

Since the system yields three products (*i.e.*, XOS, PLA, and gypsum), this study also explores the life-cycle GWP of XOS by using the economic allocation method (see ESI Fig. S1†). By using the economic allocation method, the results of scenarios 1, 2, 3, and 4 are 5.2, 15.9, 20.1, and 43.5 $kgCO_2e$ per kg, respectively. Hence, the conclusion from comparison across the four scenarios stays the same as that following the system expansion method. Except for scenario 1, the economic allocation method in the other scenarios shows −13%–14% differences compared to the system expansion method depicted in Fig. 3. In scenario 1, the discrepancy is caused principally by the low material consumption and relatively low PLA yield (see Table 5).

3.3. Life-cycle environmental impacts of XOS

Fig. 4 depicts the normalized life-cycle environmental impacts of 1 dry kg of XOS produced from poplar sawdust across the four scenarios. The normalization base for Fig. 4 is the maximum value across the four scenarios for each environmental impact category (maximum values being 100%). A total of ten impact categories are adopted, including GWP, acidification, human health – carcinogenics, human health – non-carcinogenics, eutrophication, fossil fuel depletion, ozone depletion, smog formation, ecotoxicity, and respiratory effects. The detailed absolute values of Fig. 4 before normalization are available in ESI Table S2.† The positive values of Fig. 4 represent the impacts caused by emissions, while the negative values record the potential credit provided by the byproducts (*i.e.*, PLA and gypsum) that substitute the market products.

For the total values of the four scenarios, scenario 1 shows the lowest life-cycle environmental impacts, −20%–16%, across all the impact categories. With the use of acetic acid, and increasing its concentration in pretreatment, all the life-cycle environmental impact values rise: scenario 2 ranges over 22%–37%; scenario 3 ranges over 39%–43%; scenario 4 is

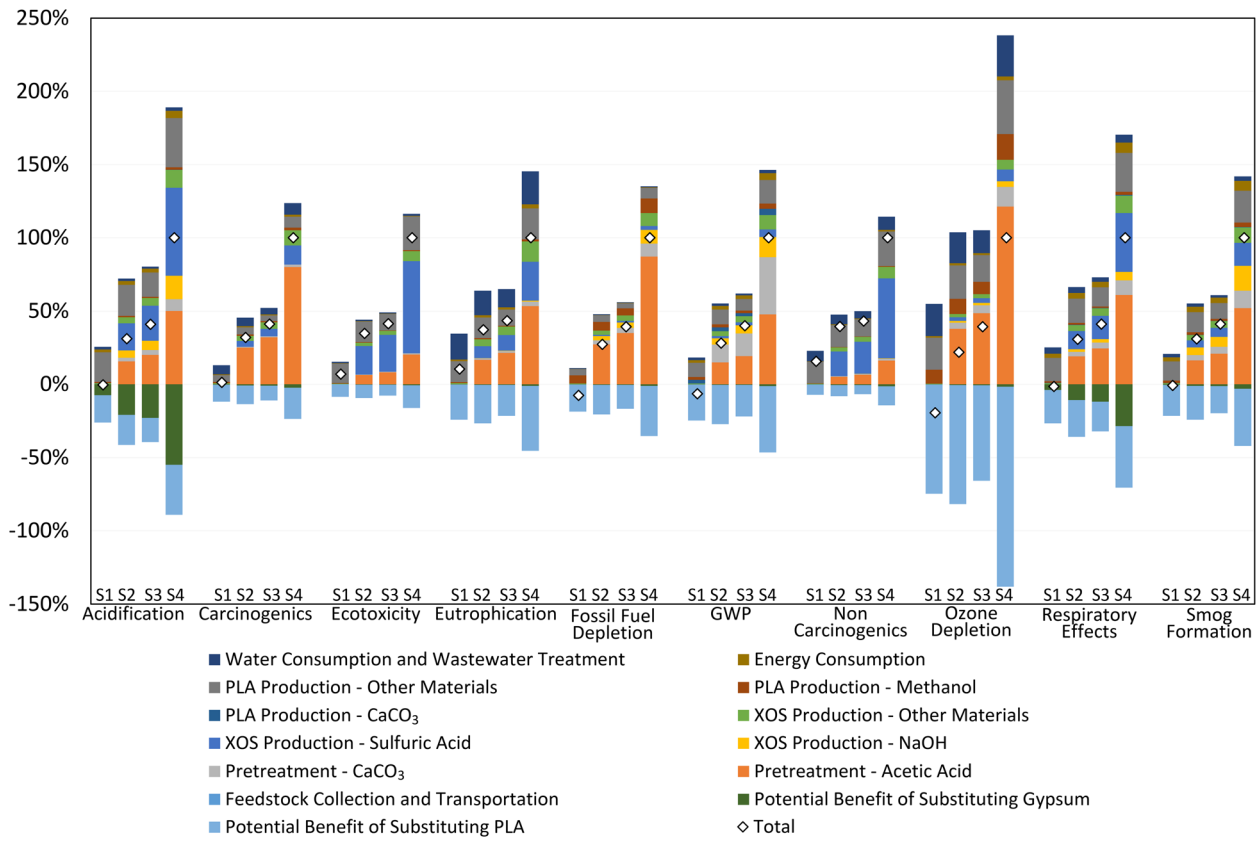

Fig. 4 The life-cycle environmental impacts of 1 kg XOS in four scenarios.

always 100%. The life-cycle results demonstrate the environmental infeasibility of deploying acetic acid during pretreatment in all ten impact categories, urging the need to discover more environmentally benign and practical chemical recovery and purification methods.

Though the comparative patterns of the total results are similar for the four scenarios, the major influences may alternate across the ten impact categories. For scenario 1, the dominant drivers are still the other materials in PLA production and the potential benefit of substituting market PLA processes. For scenarios 2–4, acetic acid in pretreatment is dominant and responsible for 45%–174% of the total life-cycle environmental impact results across all the impact categories, except ecotoxicity (18%–20%) and human health – non-carcinogenics (13%–16%). In ecotoxicity and human health – non-carcinogenics, sulfuric acid in XOS production accounts for 56%–63% and 43%–55% of the total results, respectively. This is caused by the high upstream contributions to these two impact categories from sulfuric acid. In GWP, $CaCO_3$ in pretreatment for neutralization is a major contributor due to both the upstream production and on-site emission from reactions. However, in other impact categories, $CaCO_3$ in pretreatment only accounts for 1%–19% of the total environmental impact results.

The life-cycle environmental impact results confirm that acetic acid pretreatment for XOS production indeed has obstacles in environmental aspects compared to the autohydrolysis baseline. This is primarily due to material consumption for separating and purifying the XOS-containing solution at large scale.

3.4. Life-cycle GWP of treating 1 dry t poplar sawdust

To provide an understanding of the carbon implications of various poplar sawdust treatment methods, this study also compared the life-cycle GWP of converting 1 dry t poplar sawdust to XOS with current treatment methods, namely, conventional landfill and landfill with landfill gas (LFG) recovery for power generation. Hence, all the results are represented on the 1 dry t poplar sawdust basis. Fig. 5 displays the life-cycle GWP of treating poplar sawdust in the four scenarios compared to the two landfill scenarios. The source data for Fig. 5 are available in ESI Table S3.†

As shown in Fig. 5, the landfill of 1 dry t of poplar sawdust without LFG recovery reaches 2899 $kgCO_2e$ life-cycle GWP. This is due principally to the release of methane from the landfill site and the fact that methane has a high GWP-100 factor of 27.0. In the landfill scenario without LFG recovery, the biogenic carbon in poplar sawdust is partially released as methane (~18% of carbon in poplar sawdust) and CO_2 (~19% of carbon in poplar sawdust). Hence, placing poplar sawdust in landfill without LFG recovery results in the highest GWP. If LFG recovery is implemented and recovers 75% of the methane, the net life-cycle GWP is reduced to −28 $kgCO_2e$, which also benefits from its use to generate electricity (−345 $kgCO_2e$ as the potential credit).

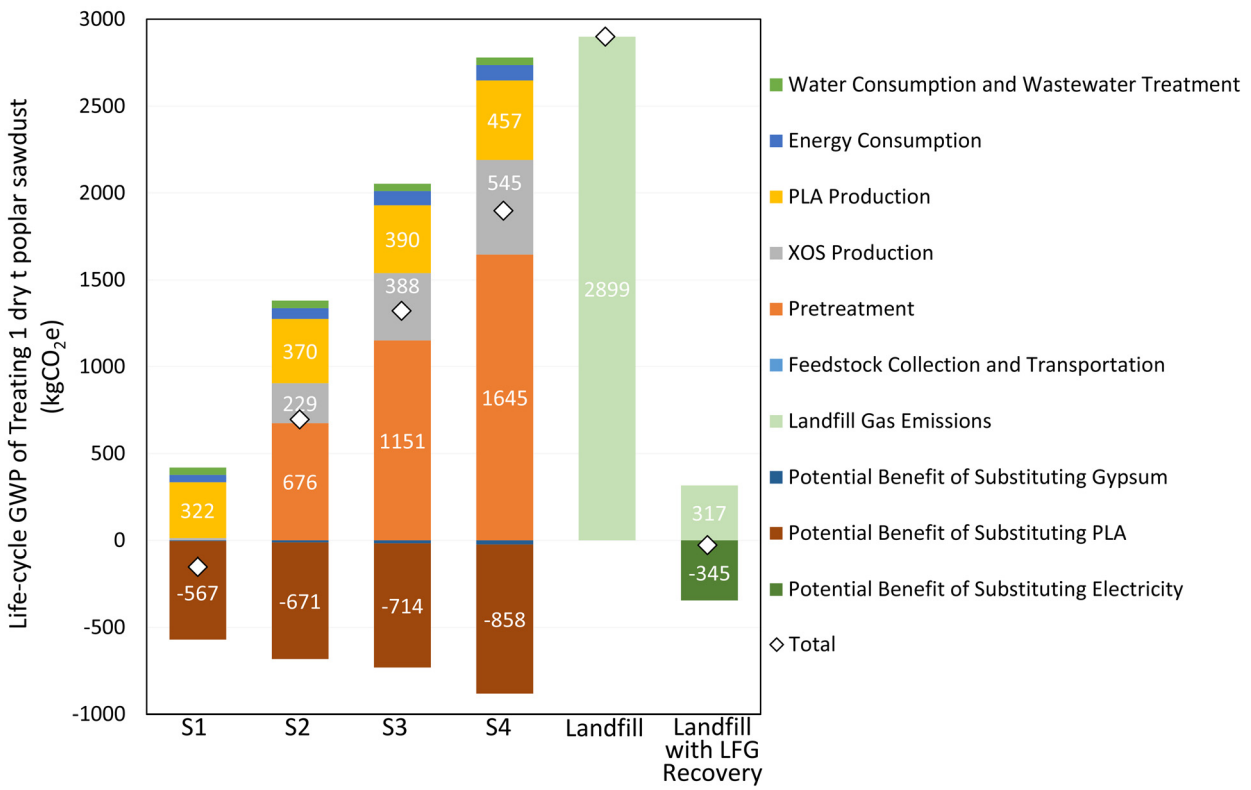

Fig. 5 The life-cycle GWP of treating 1 dry t poplar sawdust in four scenarios compared to landfill and landfill with landfill gas recovery.

In the four scenarios producing XOS, the lowest GWP still appears in scenario 1 as −152 $kgCO_2e$ per dry t poplar sawdust. With the adoption of acetic acid pretreatment, scenario 2 records 698 $kgCO_2e$ per dry t poplar sawdust, with 1322 $kgCO_2e$ in scenario 3 and 1898 $kgCO_2e$ in scenario 4. The most important determinant of the GWP is that portion of the pretreatment that features the consumption of acetic acid and $CaCO_3$. The GWP from this portion increases in proportion to the increase in acetic acid concentration, rising from 676 $kgCO_2e$ in scenario 2 to 1645 $kgCO_2e$ in scenario 4. PLA credit increases as acetic acid concentration rises, from −567 $kgCO_2e$ in scenario 1 to −858 $kgCO_2e$ in scenario 4. However, this increment of PLA credit does not sufficiently compensate for the increased GWP associated with acetic acid and $CaCO_3$ consumption. Hence, all four XOS scenarios exhibit lower GWP than landfill without LFG recovery. Only the GWP of scenario 1 is lower than that of landfill with LFG recovery. This result shows the potential environmental benefits of upcycling poplar sawdust to XOS in comparison with the current practice. However, the upcycling method with acetic acid pretreatment does not necessarily generate improved carbon benefits if landfill gas is recovered for power generation.

As this study discusses the environmental performance of XOS production under various pretreatment conditions and the feasibility of co-production of XOS and PLA, future research can conduct further techno-economic analysis (TEA) to explore the economic viability of these scenarios.[16,35,37,88,89] The TEA can investigate in particular the potential trade-offs between the environment and economic performance, and the key drivers toward economic results.

3.5. Sensitivity analysis

To investigate the impact of parameter variability and uncertainties on the results, this study conducts a sensitivity analysis for scenarios 1 and 2, representing the lowest GWP values without and with acetic acid pretreatment, respectively. Fig. 6(a) and (b) shows the sensitivity results of life-cycle GWP of scenario 1 (baseline life-cycle GWP of −3.3 $kgCO_2e$ per kg XOS) and scenario 2 (baseline life-cycle GWP of 14.0 $kgCO_2e$ per kg XOS), respectively. All the parameters vary by ±20%, unless they reach the higher limit, *e.g.*, glucose conversion rate to lactic acid in fermentation (98.0%). Based on the sensitivity analysis results, the parameters with effects of less than 2% are not displayed in Fig. 6.

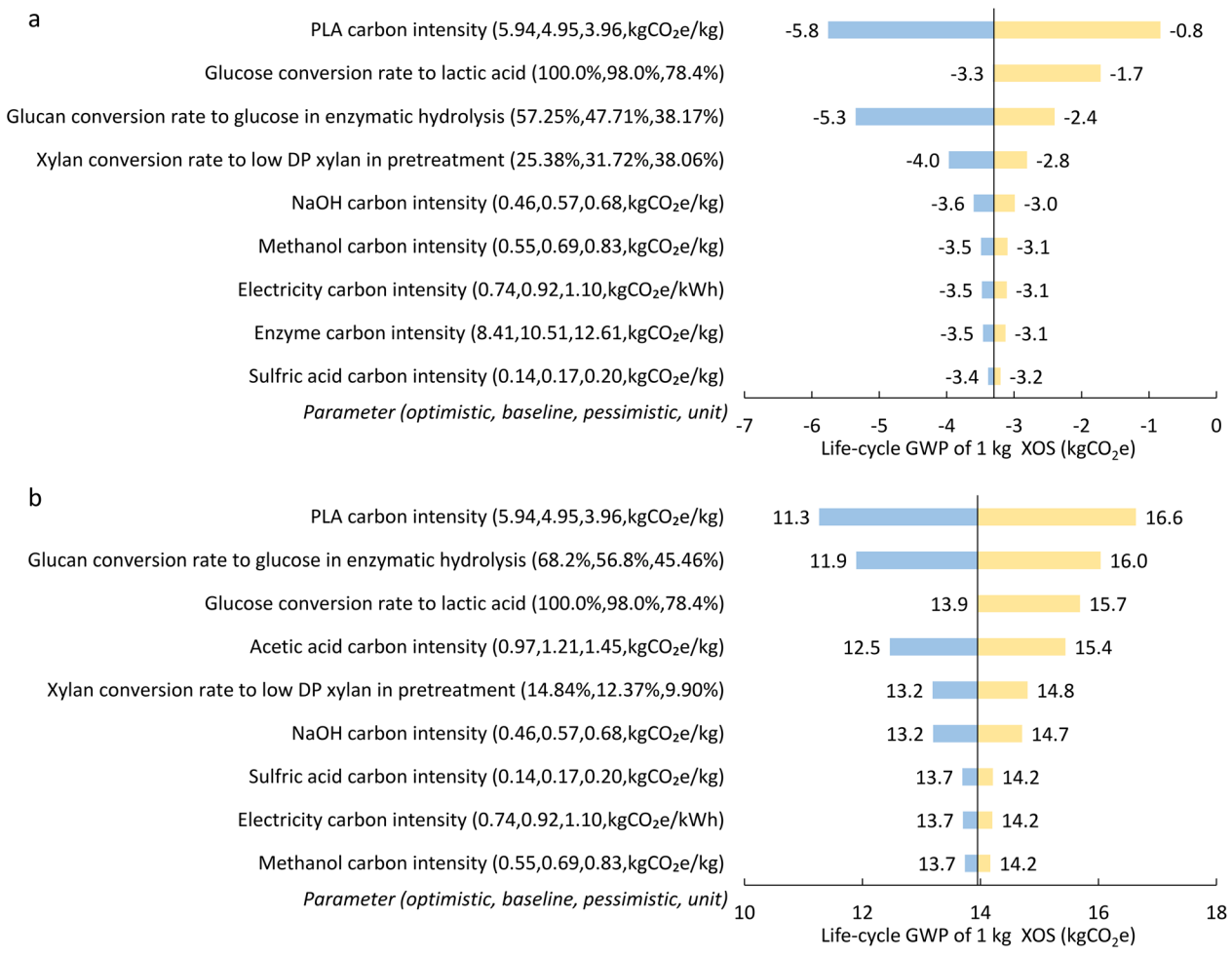

Fig. 6 The sensitivity analysis of life-cycle GWP. (a) Scenario 1; (b) scenario 2.

For scenarios 1 and 2, the carbon intensity of market PLA has the largest impact on the life-cycle GWP of XOS. The lower carbon intensity of market PLA results in lower potential substitution benefits of XOS, leading to the life-cycle GWP of XOS rising. By lowering the carbon intensity of PLA to 20%, the GWP of XOS can surge to −0.8 $kgCO_2e$ in scenario 1 and 16.6 $kgCO_2e$ in scenario 2. Two other factors directly related to PLA production also have a major impact. The first is the glucan conversion rate to glucose in enzymatic hydrolysis (later on, glucose is converted to lactic acid), while the second is the glucose conversion rate to lactic acid during fermentation. Increasing glucose yield enhances lactic acid production during fermentation, leading to higher PLA yield and greater potential substitution benefits for GWP. For example, if enzymatic hydrolysis of glucan yields 20% more glucose from glucan, the life-cycle GWP of XOS can decrease to −5.3 $kgCO_2e$ in scenario 1 and 11.9 $kgCO_2e$ in scenario 2.

Increasing the low-DP xylan yield in pretreatment can increase the final XOS yield. If the total GWP of processing 1 dry t poplar sawdust remains similar, increasing the final XOS yield will lead to the absolute value of the GWP reducing on the 1 kg XOS basis. Hence, if the total GWP of treating 1 dry t poplar sawdust is negative, increasing the low-DP xylan yield will increase the negative GWP value, as shown for scenario 1 in Fig. 6(a). In contrast, if the total GWP of treating 1 dry t poplar sawdust is positive, increasing the low-DP xylan yield will reduce the positive GWP value, as displayed for scenario 2 in Fig. 6(b). Elevating the conversion rate of xylan to low-DP xylan in pretreatment by 20% can increase the GWP of XOS to −2.8 $kgCO_2e$ in scenario 1, while this elevation can reduce the GWP of XOS to 13.2 $kgCO_2e$ in scenario 2.

As discussed above, for scenario 2 with acetic acid pretreatment, the upstream burden of acetic acid is one major contributor to the results. In Fig. 6(b), reducing the carbon intensity of acetic acid to 0.97 $kgCO_2e$ can lower the GWP of XOS by 11%. Note that the major GHG-releasing stage of $CaCO_3$ is through neutralization by reacting with acid and releasing CO_2. The upstream GWP of producing $CaCO_3$ is substantially small compared to the on-site GHG emission.[69] Other parameters, including the carbon intensity of sulfuric acid, electricity, and methanol, reveal relatively minor impacts on the final results.

4. Conclusion

This study involved conducting a cradle-to-gate LCA for the co-production of XOS and PLA from poplar sawdust in a designed large-scale biorefinery. The LCA was integrated with process models that were supported by experimental work for the key processes. The pretreatment hydrolyzes the xylan and creates the opportunity for separating the XOS and glucan that is further converted to PLA. Four scenarios are established to explore the impacts of different conditions of pretreatment with and without acetic acid. Our study indicates that the life-cycle GWP of producing 1 dry kg XOS is −3.3 $kgCO_2e$ in scenario 1 without use of acetic acid during pretreatment, 14.0 $kgCO_2e$ in scenario 2 with 3% acetic acid, 19.9 $kgCO_2e$ in scenario 3 with 5% acetic acid, and 49.9 $kgCO_2e$ in scenario 4 with 7% acetic acid. While the use of acetic acid in pretreatment increases the total XOS yield compared to no acetic acid, it also results in a higher life-cycle GWP. Trade-offs between GWP and XOS yield are identified. This phenomenon is caused principally by the upstream and on-site GHG emissions of using acetic acid and $CaCO_3$ in pretreatment, along with the materials for purifying the XOS stream in XOS production. These results highlight the necessity of conducting LCA for the process design of sustainable XOS production. For other environmental impact categories, the comparative trends emulate the results of GWP across the impact categories. This study also compares the life-cycle GWP of treating 1 dry t poplar sawdust to produce XOS and PLA, with that of placing poplar sawdust in conventional landfill and landfill with landfill gas recovery. Co-production of XOS and PLA from poplar sawdust in four scenarios achieves a lower GWP than that of placing poplar sawdust in conventional landfill. Compared to landfill with landfill gas recovery, scenario 1 without acetic acid in pretreatment can demonstrate lower GWP results. This study conducted a sensitivity analysis to assess the major drives for the life-cycle GWP of XOS. The results show that the carbon intensity of market PLA and acetic acid, glucan conversion rate to glucose in enzymatic hydrolysis, and glucose conversion rate to lactic acid are the key drivers. With practical process design and full-scale process models supported by experiment, this LCA study is able to support sustainability-informed analysis results and provide stakeholders and policy-makers with quantitative information on the carbon intensity of XOS. At the same time, this study presents suggestions on how the circular bioeconomy can contribute to climate change mitigation *via* upcycling biomass waste into high-value bioproducts.

Author contributions

C. H., Q. Y., and K. L. designed the idea. X. Z. and R. L. conducted the experimental work. K. L. conducted the LCA and sensitivity analysis. X. Z., R. L. and K. L. wrote the draft manuscript. C. H. and Q. Y. revised the manuscript. X. Z., R. L., Q. Y., C. H., and K. L. contributed to writing and finalizing the manuscript.

Conflicts of interest

The authors declare no conflicts of interest.

Data availability

All the data used and generated can be found in the text and ESI.†

Acknowledgements

X. Z., R. L., Q. Y., and C. H. are grateful for funding from the National Key Research and Development Program of China (no. 2023YFD2200505).

References

1 M. Asif and T. Muneer, *Renewable Sustainable Energy Rev.*, 2007, **11**, 1388–1413.
2 A. M. Borrero-López, C. Valencia and J. M. Franco, *Polymers*, 2022, **14**, 881.
3 X. Shen and R. Sun, *Carbohydr. Polym.*, 2021, **261**, 117884.
4 N. Singh, R. R. Singhania, P. S. Nigam, C. Di Dong, A. K. Patel and M. Puri, *Bioresour. Technol.*, 2022, **344**, 126415.
5 V. K. Garlapati, A. K. Chandel, S. P. J. Kumar, S. Sharma, S. Sevda, A. P. Ingle and D. Pant, *Renewable Sustainable Energy Rev.*, 2020, **130**, 109977.
6 A. Mirkouei, K. R. Haapala, J. Sessions and G. S. Murthy, *Renewable Sustainable Energy Rev.*, 2017, **67**, 15–35.
7 R. K. Devappa, S. K. Rakshit and R. F. H. Dekker, *Biotechnol. Adv.*, 2015, **33**, 681–716.
8 P. Sannigrahi, A. J. Ragauskas and G. A. Tuskan, *Biofuels, Bioprod. Biorefin.*, 2010, **4**, 209–226.
9 S. Zhang, X. Xu, Y. Li, X. Xie, J. Hu, S. Wu, K. Song and Q. Chu, *Ind. Crops Prod.*, 2024, **214**, 118538.
10 T. Raj, K. Chandrasekhar, A. Naresh Kumar, J. Rajesh Banu, J. J. Yoon, S. Kant Bhatia, Y. H. Yang, S. Varjani and S. H. Kim, *Bioresour. Technol.*, 2022, **344**, 126292.
11 A. A. Houfani, N. Anders, A. C. Spiess, P. Baldrian and S. Benallaoua, *Biomass Bioenergy*, 2020, **134**, 105481.
12 C. Amorim, S. C. Silvério, K. L. J. Prather and L. R. Rodrigues, *Biotechnol. Adv.*, 2019, **37**, 107397.
13 L. Santibáñez, C. Henríquez, R. Corro-Tejeda, S. Bernal, B. Armijo and O. Salazar, *Carbohydr. Polym.*, 2021, **251**, 117118.
14 P. Verma, R. Kaushik and R. Sirohi, *Biomass Convers. Biorefin.*, 2024, DOI: 10.1007/s13399-024-05993-5.
15 K. K. Valladares-Diestra, L. P. de Souza Vandenberghe, S. Vieira, L. D. Goyzueta-Mamani, P. B. G. de Mattos, M. C. Manzoki, V. T. Soccol and C. R. Soccol, *Foods*, 2023, **12**(14), 2681.
16 K. Lan, Y. Xu, H. Kim, C. Ham, S. S. Kelley and S. Park, *Bioresour. Technol.*, 2021, **340**, 125726.
17 C. de Freitas, E. Carmona and M. Brienzo, *Bioact. Carbohydr. Diet. Fibre*, 2019, **18**, 100184.
18 T. Manicardi, G. Baioni e Silva, A. A. Longati, T. D. Paiva, J. P. M. Souza, T. F. Pádua, F. F. Furlan, R. L. C. Giordano, R. C. Giordano and T. S. Milessi, *Foods*, 2023, **12**(16), 3007.
19 J. Zhao, X. Zhang, X. Zhou and Y. Xu, *Front. Bioeng. Biotechnol.*, 2021, **9**, 1–8.
20 R. Kumar, G. Næss and M. Sørensen, *J. Sci. Food Agric.*, 2024, **104**(13), 7765–7775.
21 L. Fang, Y. Su, P. Wang, C. Lai, C. Huang and Z. Ling, *Bioresour. Technol.*, 2022, **348**, 126795.
22 W. Zhang, Y. You, F. Lei, P. Li and J. Jiang, *Bioresour. Technol.*, 2018, **265**, 387–393.
23 F. S. P. P. Neto, I. U. M. Roldán, J. P. M. Galán, R. Monti, S. C. de Oliveira and F. Masarin, *Ind. Crops Prod.*, 2020, **154**, 112707.
24 P. Wen, T. Zhang, J. Wang, Z. Lian and J. Zhang, *Biotechnol. Biofuels*, 2019, **12**, 1–13.
25 B. Liu, L. Liu, B. Deng, C. Huang, J. Zhu, L. Liang, X. He, Y. Wei, C. Qin, C. Liang, S. Liu and S. Yao, *Int. J. Biol. Macromol.*, 2022, **222**, 1400–1413.
26 H. Zhang, Y. Xu and S. Yu, *Bioresour. Technol.*, 2017, **234**, 343–349.
27 X. Zhou and Y. Xu, *Bioresour. Technol.*, 2019, **282**, 81–87.
28 N. I. Wan Azelee, J. M. Jahim, A. F. Ismail, S. F. Z. M. Fuzi, R. A. Rahman and R. Md Illias, *Ind. Crops Prod.*, 2016, **81**, 11–19.
29 J. Li, Y. Wang, C. Xu, S. Liu, J. Dai and K. Lan, *Sci. Total Environ.*, 2024, **946**, 174349.
30 Y. Wang and K. Lan, *Clean. Environ. Syst.*, 2024, **15**, 100243.
31 ISO, *ISO 14040:2006 Environmental management—Life cycle assessment—Principles and framework*, 2006.
32 K. Lan, B. Zhang and Y. Yao, *Joule*, 2024, 1–20.
33 K. Lan, H. S. Wang, T. Lee, C. A. De Assis, R. A. Venditti, Y. Zhu and Y. Yao, *Green Chem.*, 2024, **26**(6), 3466–3478.
34 Y. Yao, K. Lan, T. E. Graedel and N. D. Rao, *Annu. Rev. Chem. Biomol. Eng.*, 2024, **15**, 1–23.
35 C. van Heerden, S. Farzad and J. F. Görgens, *ACS Sustainable Chem. Eng.*, 2023, **11**, 16453–16468.
36 S. González-García, P. C. Morales and B. Gullón, *Ind. Crops Prod.*, 2018, **123**, 331–340.
37 T. F. Lopes, F. Carvalheiro, L. C. Duarte, F. Gírio, J. A. Quintero and G. Aroca, *Biofuels, Bioprod. Biorefin.*, 2019, **13**, 1321–1332.
38 S. Engelmann, *POLY (LACTIC ACID) Synthesis, Structures, Properties, Processing, Applications, and End of Life*, 2022.
39 Z. Shi, L. Liu, H. Chen, C. Tang, J. Yu and Y. Fan, *Carbohydr. Polym.*, 2024, **323**, 121369.
40 R. Li, Y. Zheng, C. Huang and K. Lan, *Chem. Eng. Sci.*, 2025, **302**, 120804.
41 Y. Su, L. Fang, P. Wang, C. Lai, C. Huang, Z. Ling and Q. Yong, *Bioresour. Technol.*, 2022, **358**, 127365.
42 K. Huang, J. Luo, R. Cao, Y. Su and Y. Xu, *J. Wood Chem. Technol.*, 2018, **38**, 371–384.
43 Y. Su, L. Fang, P. Wang, C. Lai, C. Huang, Z. Ling, S. Sun and Q. Yong, *Bioresour. Technol.*, 2021, **342**, 125955.
44 Y. Su, P. Wang, C. Lai, C. Huang, Z. Ling and Q. Yong, *Ind. Crops Prod.*, 2023, **194**, 116297.
45 D. Humbird, R. Davis, L. Tao, C. Kinchin, D. Hsu, A. Aden, P. Schoen, J. Lukas, B. Olthof, M. Worley, D. Sexton and D. Dudgeon, *Process design and economics for biochemical conversion of lignocellulosic biomass to ethanol: dilute-acid pretreatment and enzymatic hydrolysis of corn stover (no. NREL/TP*-5100-47764), Golden, CO, 2011.

46 ISO, *ISO 14044: Environmental Management, Life Cycle Assessment, Requirements and Guidelines*, 2006.
47 J. B. Dunn, F. Adom, N. Sather, J. Han and S. Snyder, *Life-cycle analysis of bioproducts and their conventional counterparts in GREET*, 2015.
48 J. Zheng and L. Rehmann, *Int. J. Mol. Sci.*, 2014, **15**, 18967–18984.
49 W. Lin, J. Yang, Y. Zheng, C. Huang and Q. Yong, *Biotechnol. Biofuels*, 2021, **14**, 1–15.
50 P. Moura, R. Barata, F. Carvalheiro, F. Gírio, M. C. Loureiro-Dias and M. P. Esteves, *LWT – Food Sci. Technol.*, 2007, **40**, 963–972.
51 J. S. Gütsch and H. Sixta, *Holzforschung*, 2011, **65**, 511–518.
52 C. Huang, C. Lai, X. Wu, Y. Huang, J. He, C. Huang, X. Li and Q. Yong, *Bioresour. Technol.*, 2017, **241**, 228–235.
53 W. Deesukon, Y. Nishimura, T. Sakamoto and W. Sukhumsirichart, *Mol. Biotechnol.*, 2013, **54**, 37–46.
54 Q. P. Yuan, H. Zhang, Z. M. Qian and X. J. Yang, *J. Chem. Technol. Biotechnol.*, 2004, **79**, 1073–1079.
55 A. A. Aachary and S. G. Prapulla, *Compr. Rev. Food Sci. Food Saf.*, 2011, **10**, 2–16.
56 F. K. Adom and J. B. Dunn, *Biofuels, Bioprod. Biorefin.*, 2017, **11**, 258–268.
57 P. Walsh and J. Venus, WO2013164423A1, 2013.
58 P. B. Yang, Y. Tian, Q. Wang and W. Cong, *Biochem. Eng. J.*, 2015, **98**, 38–46.
59 W. J. Groot and T. Borén, *Int. J. Life Cycle Assess.*, 2010, **15**, 970–984.
60 J. Sadhukhan, E. Martinez-Hernandez, M. A. A. Allieri, J. A. Z. Eguía-Lis, A. Castillo, D. Dominguillo, E. Torres-García and J. Aburto, *J. Cleaner Prod.*, 2024, **434**, 140386.
61 A. Morão and F. de Bie, *J. Polym. Environ.*, 2019, **27**, 2523–2539.
62 J. Sadhukhan, K. S. Ng and E. M. Hernandez, *Biorefineries and Chemical Processes: Design, Integration and Sustainability Analysis*, John Wiley & Sons, 2014.
63 E. T. H. Vink, K. R. Rábago, D. A. Glassner and P. R. Gruber, *Polym. Degrad. Stab.*, 2003, **80**, 403–419.
64 T. Kim, A. Bhatt, L. Tao and P. T. Benavides, *J. Cleaner Prod.*, 2022, **380**, 135110.
65 S. S. Bapat, C. P. Aichele and K. A. High, *Sustainable Chem. Processes*, 2014, **2**, 1–8.
66 S. P. Kamble, P. P. Barve, J. B. Joshi, I. Rahman and B. D. Kulkarni, *Ind. Eng. Chem. Res.*, 2012, **51**, 1506–1514.
67 M. Singhvi and D. Gokhale, *RSC Adv.*, 2013, **3**, 13558–13568.
68 R. Davis, L. Tao, E. C. D. Tan, M. J. Biddy, G. T. Beckham, C. Scarlata, J. Jacobson, K. Cafferty, J. Ross, J. Lukas, D. Knorr and P. Schoen, *Process Design and Economics for the Conversion of Lignocellulosic Biomass to Hydrocarbons: Dilute-Acid and Enzymatic Deconstruction of Biomass to Sugars and Biological Conversion of Sugars to Hydrocarbons*, 2013.
69 G. Wernet, C. Bauer, B. Steubing, J. Reinhard, E. Moreno-Ruiz and B. Weidema, *Int. J. Life Cycle Assess.*, 2016, **21**, 1218–1230.
70 Argonne National Laboratory, *The greenhouse gases, regulated emissions, and energy use in technologies (GREET) model*, 2022.
71 F. C. Barbosa, G. P. Nogueira, E. Kendrick, T. T. Franco, D. Leak, M. O. S. Dias, C. K. N. Cavaliero and R. Goldbeck, *Biofuels, Bioprod. Biorefin.*, 2021, **15**, 1763–1774.
72 S. Zhou, X. Zhou, X. Hua, Q. Yong, D. Liu and Y. Xu, *Biocatal. Agric. Biotechnol.*, 2024, **60**, 103297.
73 Kangwei Biologic Co. Ltd, Kangweisu XOS.
74 ChemAnalyst, Polylactic Acid (PLA) Price Trend and Forecast, **https://www.chemanalyst.com/Pricing-data/polylactic-acid-1275**.
75 USA Gypsum, Fine gypsum price, **https://www.usagypsum.com/**.
76 S. Towprayoon, T. Ishigaki, C. Chiemchaisri, A. O. Abdel-Aziz, M. E. Hunstone, C. Jarusutthirak, M. Ritzkowski and M. Thomsen, in *2019 Refinement to the 2006 IPCC Guidelines for National Greenhouse Gas Inventories*, 2019, vol. 5, pp. 6.1–6.49.
77 US EPA, Landfill Methane Outreach Program (LMOP), **https://www.epa.gov/lmop/project-and-landfill-data-state**.
78 M. Anshassi, H. Sackles and T. G. Townsend, *Resour., Conserv. Recycl.*, 2021, **174**, 105810.
79 IPCC, *Climate Change 2021: The Physical Science Basis AR 6 Work Group I*, 2022.
80 M. Ryberg, M. D. M. Vieira, M. Zgola, J. Bare and R. K. Rosenbaum, *Clean Technol. Environ. Policy*, 2014, **16**, 329–339.
81 H. Liao, Z. Chen, P. Wen, W. Ying and J. Zhang, *Ind. Crops Prod.*, 2023, **205**, 117497.
82 X. Hao, F. Xu and J. Zhang, *Carbohydr. Polym.*, 2022, **285**, 119217.
83 X. Zhao, Q. Wang, T. Wang, Y. Su, C. Huang, C. Lai and Q. Yong, *Food Bioprod. Process.*, 2024, **143**, 202–211.
84 H. O. M. A. Moura, L. M. A. Campos, V. L. da Silva, J. C. F. de Andrade, S. M. N. de Assumpção, L. A. M. Pontes and L. S. de Carvalho, *Cellulose*, 2018, **25**, 5669–5685.
85 S. Şahin and E. Kurtulbaş, *Biomass Convers. Biorefin.*, 2022, **12**, 341–349.
86 L. de Oliveira Carneiro, R. P. D. S. Matos, W. B. Ramos, R. P. Brito and K. D. Brito, *Chem. Eng. Process.*, 2022, **181**, 109176.
87 P. Pal and J. Nayak, *Sep. Purif. Rev.*, 2017, **46**, 44–61.
88 W. G. Sganzerla, M. F. da Silva, G. L. Zabot, R. Goldbeck, S. I. Mussatto and T. Forster-Carneiro, *J. Supercrit. Fluids*, 2023, **196**, 105895.
89 L. J. Swart, A. M. Petersen, O. K. K. Bedzo and J. F. Görgens, *J. Chem. Technol. Biotechnol.*, 2021, **96**, 1632–1644.